Journal of Molecular Catalysis A: Chemical 372 (2013) 72–78

Contents lists available at SciVerse ScienceDirect

Journal of Molecular Catalysis A: Chemical

journal homepage: www.elsevier.com/locate/molcata

Dioxygen oxidation of 1-phenylethanol with gold nanoparticles and *N*-hydroxyphthalimide in ionic liquid

Hassan Hosseini-Monfared*[,1], Hajo Meyer, Christoph Janiak*

Institut für Anorganische Chemie und Strukturchemie, Universität Düsseldorf, Universitätsstr. 1, D-40225 Düsseldorf, Germany

ARTICLE INFO

Article history:
Received 30 November 2012
Received in revised form 10 February 2013
Accepted 11 February 2013
Available online xxx

Keywords:
Gold nanoparticles
Oxidation catalysis
Dioxygen
Ionic liquids
Alcohol

ABSTRACT

Gold nanoparticles (Au-NPs) of 8 nm average diameter were obtained by thermal reduction under nitrogen from $KAuCl_4$ in the presence of *n*-butylimidazol dispersed in the ionic liquid (IL) 1-*n*-butyl-3-methylimidazolium tetrafluoroborate ($BMIm^+BF_4^-$). Characterization of the Au-NP was done by transmission electron microscopy (TEM) and dynamic light scattering (DLS). Catalytic activities of the Au-NP/IL dispersion were evaluated in the oxidation of 1-phenylethanol at 100 and 160 °C under 4 bar pressure of dioxygen in a base-free system. Au-NP in combination with the radical initiator *N*-hydroxyphthalimide (NHPI) showed good conversion and selectivity for the oxidation of 1-phenylethanol to acetophenone through formation of an α-hydroxy carbon radical. The concomitant side products di(1-phenylethyl)ether and di(1-phenylethyl)peroxide were rationalized by an equilibrium due to the IL matrix of the α-hydroxy carbon radical with the 1-phenylethoxy radical. Maximum turnover number was ~5200 based on the total number of moles of gold but a factor of about six larger, TON ≈ 31 300, when only considering the Au-NP surface atoms. The fraction (N_S/N_T) of exposed surface atoms ($N_S \approx 2560$) for an average 8 nm Au-NP (having $N_T \approx 15\,800$ atoms in a ~17-shell icosahedral or cuboctahedral particle) was estimated here as 0.16.

1. Introduction

Selective oxidation of alcohols to carbonyl compounds is a fundamental transformation in organic synthesis because the target molecules can be obtained directly in one-pot sequences. Alcohols are important precursors for various chemicals and in particular, the oxidation of alcohols and polyols is of interest owing to the large array of biological hydroxy-derivatives [1–3]. Choice of the oxidants determines the practicability and efficiency of the oxidation reactions. Oxidants, like MnO_4^- and $Cr_2O_7^{2-}$ produce toxic, environmentally and economically unacceptable by-products or like NaOCl have a low (≤30 wt.%) active oxygen content. In this context, O_2 (or air) is the most attractive oxidants because of its high contents of active oxygen species (100% for dioxygenase-type, 50% for monooxygenase-type) and co-production of only water.

Nanoparticles (NPs) are of high interest in catalysis [4–6]. The small size of nanoparticles results in a large fraction of surface atoms [7]. Interaction of unprotected small particles will, however lead to agglomeration or aggregation from the cohesive surface energy [8]. As a result of their colloidal instability, many nanoparticles need to be stabilized via additional (capping) agents such as surfactants or polymers, which provide a steric, electrostatic or electrosteric particle stabilization [9]. For catalytic applications of NPs strong surface protection is, however, undesirable as it hinders substrate access and interaction with the surface catalytic sites. Instead ligand-free NPs should be advantageous for a high activity. Ionic liquids (ILs) can stabilize M-NPs on the basis of their ionic nature [10], high polarity, high dielectric constant and supramolecular network without the need of additional protective ligands [11]. ILs can therefore function both as stabilizer and solvent for the preparation of small (<5 nm) and (generally) kinetically stabilized M-NPs [4,12,13].

The past decade has seen an explosive growth in catalytic reactions studied in ILs. Often the IL enables more efficient reactions compared with standard organic solvents and catalysts show good or even enhanced activities when applied in ionic liquids [14–16]. ILs are interesting in the context of green catalysis [17] which requires that catalysts be designed for easy product separation from the reaction products and multi-time efficient reuse/recycling [18]. The Pd-metal-catalyzed oxidation of benzyl alcohol with 1 atm O_2 in the IL $BMIm^+X^-$ gave good conversion to benzaldehyde, albeit only for X = BF_4 and not for X = Cl or Br and with Pd amounts of equal or larger than 2.8 mol% [19].

Oxidation by gold is of timely interest for green processes requiring stable, selective and non-toxic heterogeneous catalysts, as well

* Corresponding authors. Tel.: +49 2118112286.
E-mail addresses: monfared@znu.ac.ir (H. Hosseini-Monfared), janiak@uni-duesseldorf.de (C. Janiak).
[1] Permanent address: Department of Chemistry, University of Zanjan, 45195 313, Zanjan, Iran.

1381-1169/$ – see front matter © 2013 Elsevier B.V. All rights reserved.
http://dx.doi.org/10.1016/j.molcata.2013.02.007

as air or O_2 as oxidants [20–22]. Gold is cheaper than platinum, palladium and most other noble metals used as catalyst. One of the unique features of gold catalysis is the kinetic aspect of correlating the turnover frequency strongly to the size of metallic gold particles. In particular, many investigations on the liquid-phase oxidation of polyols, alcohols and carbohydrates indicate that only small gold particles are catalytically active [23]. A size threshold in gold catalytic activity has been found resulting in complete inactivity for particles with diameters >∼2 nm [20]. Compared to other common catalysts, like the platinum group metals, the outstanding properties of gold catalysis are also represented by high selectivity which allows discrimination within chemical groups and geometrical positions, leading to superior yields in the desired products. Among many examples, glycols can be oxidized to monocarboxylates [24], and unsaturated alcohols to unsaturated aldehydes [25]. From its biocompatibility, availability and easy recovery, gold appears as an exciting catalyst for sustainable processes based on the use of clean reagents, particularly O_2. Considering the influence of various parameters in the aerobic oxidation of alcohols by gold based catalysts, it can be concluded that a prominent role in the activity and selectivity is played by the solvent [26].

Unsupported nanogold was described for the aerobic oxidation of stilbene and cyclohexene in methylcyclohexane [27] and the aerobic oxidation of alcohols [28]. Gold nanoparticles have been used mostly as supported catalysts for oxidation applications [14,20,30,29,26]. The unique catalytic activity of supported Au nanoparticles has been ascribed to various effects including thickness/shape, the metal oxidation state, and support effects [31]. Benzyl alcohol is oxidized selectively to benzaldehyde with high yield by molecular oxygen over a reusable nano-sized gold catalyst supported on U_3O_8, MgO, Al_2O_3 or ZrO_2 in the absence of any solvent with only little formation of benzylbenzoate [32].

From the viewpoints of atom economy and environmental concern, developing noble metal catalysts and using molecular oxygen or air as the oxidant prevail as an attractive green technology [33,34]. Here we report to the best of our knowledge for the first time oxidation of an alcohol with gold nanoparticles (Au-NPs) in an ionic liquid (Scheme 1).

2. Experimental

2.1. Materials and instrumentation

$KAuCl_4$ was obtained from STREM, *n*-butylimidazole (p.a.) from Aldrich, *N*-hydroxyphthalimide (NHPI) from ACROS, the ionic liquid (IL) 1-*n*-butyl-3-methylimidazolium tetrafluoroborate ($BMIm^+BF_4^-$) from IoLiTec (H_2O content ≪ 100 ppm; Cl^- content ≪ 50 ppm). All manipulations were done by using Schlenk techniques under nitrogen. The ionic liquid was dried under a high vacuum (10^{-3} mbar) for several days to avoid hydrolysis of $BMIm^+BF_4^-$ to HF [18,35–37].

FT-IR (Fourier transform infrared) measurements were carried out on a Bruker TENSOR 37 IR spectrometer in a range from 4000 to 500 cm^{-1} with ATR technique.

A Malvern Zetasizer Nano-ZS was used for the dynamic light scattering (DLS) measurements working at 633 nm wavelength. The resolution of the DLS instrument is 0.6 nm. Care was taken for choosing the right parameters, such as the index of refraction of Au (0.11) with absorption of 0.1 at this wavelength. Samples were prepared by dilution of the metal/IL dispersion (10 μL; 1.0 wt.% of Au) in *n*-butylimidazole (2 mL, 99% p.a.; particle free) and was placed in a glass cuvette before measurement.

HAADF-STEM (high angle annular dark field scanning transmission electron microscopy) images were taken with FEI TECNAI G^2 F 20 (S)TEM and FEI TITAN 80-300 probe CS-corrected STEM. All samples for HAADF-STEM were prepared by dropping a small amount of Au-NP/IL dispersion on a carbon coated copper grid. After 5 min the excess of the IL was removed by dipping the grid into a water bath for 2 min. Finally the grid was plasma cleaned for 10 s.

Gas chromatography measurements were conducted using a Perkin Elmer headspace GC HS6 with a flame ionization detector (FID) and a PEG capillary column (25 m long × 0.32 mm inner diameter × 1.0 μm film thickness). The GC program used was: oven temperature 120 °C, injector temperature 170 °C, carrier gas N_2 pressure 200 kPa. The conversion was analyzed by adding a drop of the mixture into a headspace GC sample vial with 1 mL of water. The addition of water as a non-electrolyte can enlarge the activity coefficient of organic components; thereby increases their detection sensitivity through the increase in peak area. The FID does not detect the water itself [38]. In order to verify the results of the headspace GC analyses we isolated the reaction products from selected experiments using standard procedures and confirmed their purity by ^1H NMR. Conversion and selectivity were calculated with respect to the substrate. The products were identified with Thermo Trace DSQ GC-MS and ^1H NMR. ^1H NMR spectra were collected on a Bruker Avance DRX 500 spectrometer (500 MHz) or a Bruker Avance DRX 200 spectrometer (200 MHz) as $CDCl_3$ solutions.

2.2. Synthesis of gold nanoparticles in ILs [12]

Au-NP was prepared by thermal decomposition and reduction from $KAuCl_4$ in an ionic liquid (cf. Scheme 1) under nitrogen in a glass vessel which was connected to an oil bubbler. In a typical experiment $KAuCl_4$ (57.6 mg, 0.152 mmol) was dissolved/dispersed (during 48 h) under nitrogen at room temperature in the presence of *n*-butylimidazole (1.5 equiv. for each Cl atom, 0.914 mmol) in the ionic liquid 1-*n*-butyl-3-methylimidazolium tetrafluoroborate ($BMIm^+BF_4^-$) (3.0 g, 2.5 mL, density 1.2 g/mL). The solution was slowly heated to 230 °C for 18 h under magnetic stirring. The solution color immediately changed from yellow to dark red (dark brown-red), indicating the formation of gold nanoparticles. The decomposition process gave a 1.0 wt.% or 60.8 μmol/mL dispersion of gold (30 mg in 3.0 g IL). During the decomposition process, a white haze of *n*-butylimidazolium chloride was formed. After cooling to room temperature under nitrogen, an aliquot of the ionic liquid was collected under nitrogen atmosphere for TEM and dynamic light scattering (DLS) characterization.

2.3. Catalytic dioxygen oxidation of alcohol with Au-NP/IL

The oxidation reactions were carried out in a glass inlay of a 100 mL steel autoclave. The autoclave was conditioned by evacuation and re-filling with dioxygen. All autoclave loading was carried out under air. In a typical experiment, 5.0 mL (41.3 mmol) of 1-phenylethanol was added to the reactor with 0.1 mL Au-NP/$BMIm^+BF_4^-$ dispersion (6.1 μmol Au) and NHPI (1 mmol). After purging with O_2, the reactor was pressurized to 4 bar and placed in a thermostated oil bath at a chosen temperature of 100 or 160 °C (see Table 1). Stirring rate was 850 rpm. The O_2 consumption over time was monitored online with a Büchi pressflow gas controller (Büchi pbc). After 24 h the reactor was depressurized and the product mixture was analyzed by gas chromatography and ^1H NMR as follows: (i) by taking a sample with a Pasteur-pipette from the reaction mixture without removing the NP/IL dispersion and after adding 1 mL water injecting it into headspace GC; (ii) by evacuating the substrate/product from the NP/IL under vacuum (0.003 mbar, 200 °C) into a clean cold trap and injecting into headspace GC; (iii) by removing the substrate/product from NP/IL by extraction with petroleum ether or diethyl ether (3× 1 mL) and

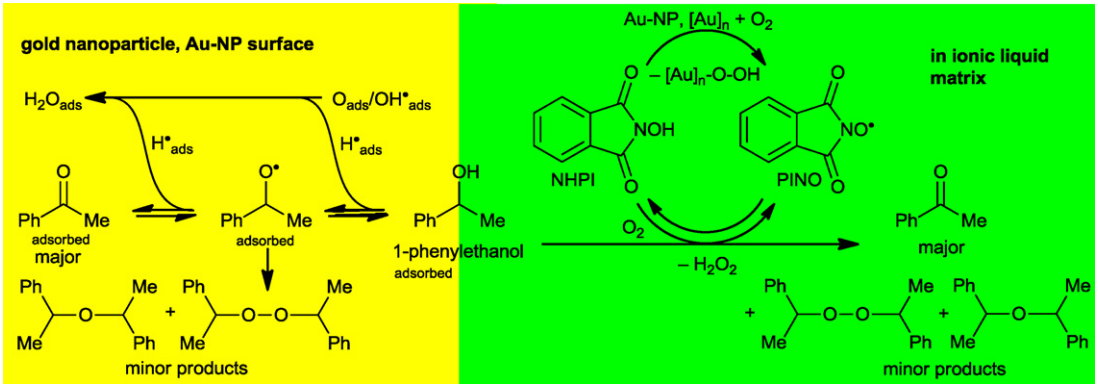

Scheme 1. Summary of the work reported here with two catalytic mechanisms depending on Au-NP/IL or Au-NP/IL/NHPI catalysis (Au-NP = gold nanoparticle, IL = ionic liquid, NHPI = *N*-hydroxyphthalimide, PINO = phthalimide *N*-oxyl (PINO) radical).

Table 1
Oxidation of 1-phenylethanol with Au-NP and O_2.[a]

No.	Catalyst	Temp. (°C)	Conversion			Products (selectivity%)[b]		
			(%)	TON[c]	$TON_{surface}$[d]	Acetophenone	~Ether	~Peroxide
1	None	100	No reaction					
2	NHPI	100	12			100	–	–
3	Au-NP/IL	100	3	200	1200	100	–	–
4	Au-NP/IL[e]	100	2	70	420	100	–	–
5	Au-NP/IL/NHPI	100	13	880	5280	69	15	15
6	Au-NP/IL/NHPI	100	60[f]	810	4860	47	27	27
7	None	160	31			74	13	13
8	NHPI	160	44			86	7	7
9	Au-NP/IL	160	50	3390	20 340	68	16	16
10	Au-NP/IL[g]	160	43	970	5820	61	19	19
11	Au-NP/IL/NHPI	160	77	5220	31 320	58	29	14
12	Au-NP/IL[h]/NHPI	160	69	940	5640	48	28	25

[a] Conditions: catalyst 0.1 mL Au-NP/IL dispersion (6.1 μmol Au), 5.0 mL 1-phenylethanol (41.35 mmol) giving a molar substrate/Au ratio of 6780, O_2 pressure 4 bar, NHPI (*N*-hydroxyphthalimide) 1 mmol, reaction time 24 h, unless noted otherwise. Each catalytic reaction was carried out at least twice to ensure reproducibility.
[b] Products were acetophenone, di(1-phenylethyl)ether $Ph(CH_3)CH—O—CH(CH_3)Ph$ and di(1-phenylethyl)peroxide $Ph(CH_3)CH—O—O—CH(CH_3)Ph$.
[c] TON = mol(products)/mol(Au) for the conversion reached after 24 h.
[d] $TON_{surface}$ = [mol(products)/mol(Au)]/(N_S/N_T) with the fraction of surface atoms $N_S/N_T = 0.16$ or ~1/6 (see estimation in text).
[e] 0.2 mL Au-NP/IL dispersion, 12.2 μmol Au, molar substrate/Au ratio = 3390.
[f] 1.0 mL 1-phenylethanol (8.27 mmol), molar substrate/Au ratio = 1356.
[g] 0.3 mL Au-NP/IL dispersion, 18.3 μmol Au, molar substrate/Au ratio = 2260.
[h] 0.5 mL Au-NP/IL, 30.5 μmol Au, molar substrate/Au ratio = 1356.

injecting the into headspace-GC. The reaction mixture (organic phase + NP/IL) could also easily be analyzed by ^{1}H NMR without separation of NP/IL (see Fig. S1 in supporting information). In the ^{1}H NMR spectrum of the reaction mixture there was no overlap between substrates/products and IL peaks. This way it was also ensured that no product was lost or the substrate/product ratio changed due to distillation or extraction. Alternatively, for ^{1}H NMR analysis the substrate/product can be separated from the NP/IL by extraction with diethyl ether (3× 1 mL) which is also preferred in order to try to reuse the NP/IL.

To ensure reproducibility each catalytic reaction was carried out at least twice.

3. Results and discussion

Gold nanoparticles with an average diameter of 8 nm (Figs. 1 and 2) were produced in the ionic liquid 1-*n*-butyl-3-methylimidazolium tetrafluoroborate ($BMIm^+BF_4^-$) as reported in the literature (Scheme 1) [12]. The synthesis of Au-NP was carried out under nitrogen in a Schlenk vessel in the carefully dried and deoxygenated ionic liquid. Upon exposure to air, the yellow-orange Au dispersion in $BMIm^+BF_4^-$ forms a red-purple precipitate, indicating particle aggregation. Without the presence of *n*-butylimidazole the Au-NP/IL dispersion also quickly turns red-purple, indicating an agglomeration process which is presumably caused by the generated free HCl acid (cf. Scheme 1). In the absence of air, Au-NP are effectively stabilized by the IL without the need of additional capping ligands [12]. When 0.1 mL of the Au-NP/IL dispersion was added to 5 mL of 1-phenylethanol for the catalytic reaction (see below) no precipitation was detectable in the presence of air and after a 24 h reaction at 100 or 160 °C.

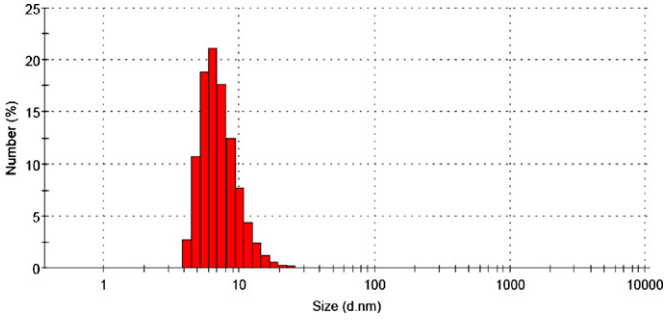

Fig. 1. Example of a histogram of the number-size-distribution for Au-NP (synthesized as 1 wt.% in $BMIm^+BF_4^-$) from dynamic light scattering (DLS) with medium diameter (hydrodynamic diameter with standard deviation σ) of (8 ± 2) nm from 10 measurements.

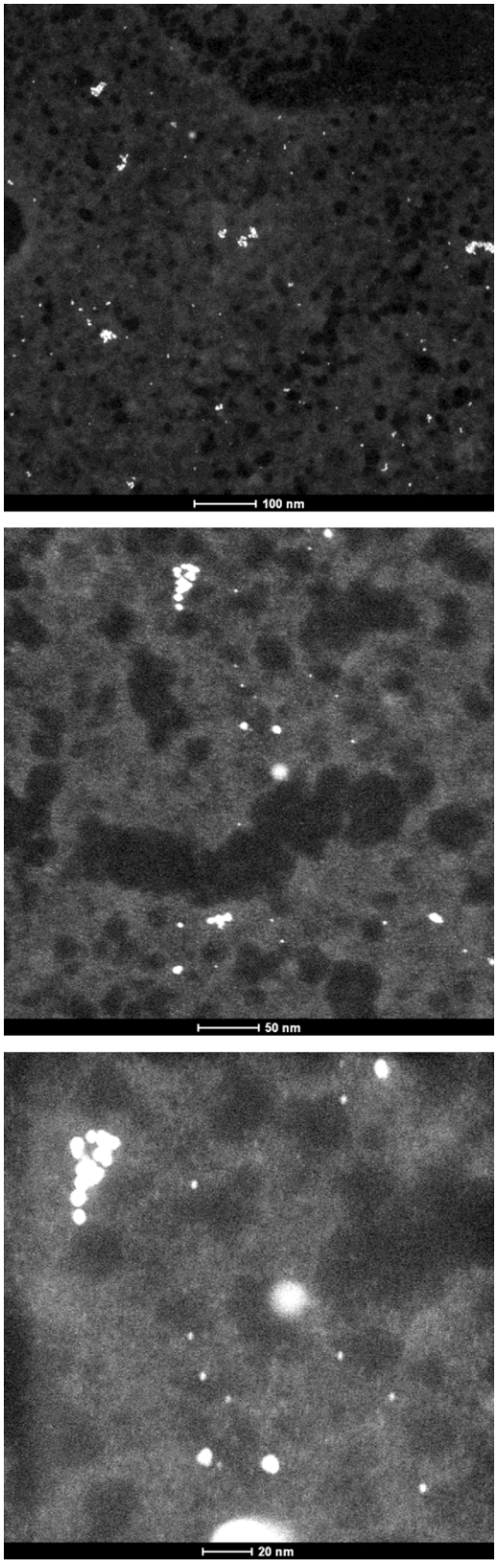

Fig. 2. Examples of high-angle annular dark field scanning transmission electron microscopy (HAADF-STEM) images of Au-NP in $BMIm^+BF_4^-$. Particle size determination from TEM gave an average diameter (8 ± 3) nm. The larger bright spot near the center in the middle and bottom TEM pictures arises from the focused electron beam during the image scan. This is clearly illustrated with the zoomed-in TEM at the bottom, where the bright near-center spot was not yet present in the middle TEM picture.

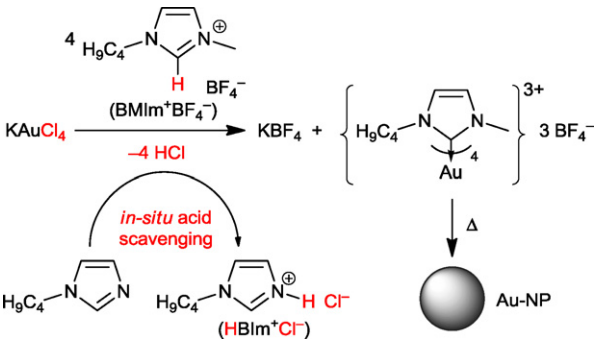

Scheme 2. Formation of Au nanoparticles by thermal decomposition and reduction of $KAuCl_4$ in the IL $BMIm^+BF_4^-$. The formed $BHIm^+Cl^-$ was analyzed by elemental analysis and ^1H NMR. Au-NP formation is suggested through the formation of an Au–carbene intermediate with subsequent reductive decomposition.

As for Pd-NPs, we suggest here the formation of *N*-heterocyclic carbene (NHC)–Au species as the origin of the formation of Au-NP (Scheme 2) [39,40]. We also suggest that the formation of these Au–NHC intermediates slows down the aggregation process. In the presence of *n*-butylimidazole, the released HCl is bound as an imidazolium salt (precipitating as a white haze), similar to the IL matrix. This prevents the formation of an acidic reaction medium, which would destabilize the Au-NP and lead to clustering.

3.1. Catalytic activities of Au-NP

The Au-NP catalytic potential was evaluated in the oxidation of 1-phenylethanol with dioxygen under pressure of 4 bars. Auto oxidation of 1-phenylethanol was not observed under 4 bar pressure of dioxygen at 100 °C (Table 1, entry 1). However, in the presence of the radical initiator *N*-hydroxyphthalimide (NHPI) the alcohol was oxidized with 12% conversion after 24 h (Table 1, no. 2). Oxidation of 1-phenylethanol by using low or high concentration of Au-NP in IL alone (6.1 μmol, 12.2 μmol) occurred with 100% selectivity to acetophenone but the conversion (2–3%) was very low (Table 1, nos. 3 and 4).

Au-NP/IL with the radical initiator NHPI increased the conversion only upon lowering the alcohol substrate to gold ratio. In addition the combination of Au-NP/IL with NHPI decreased the

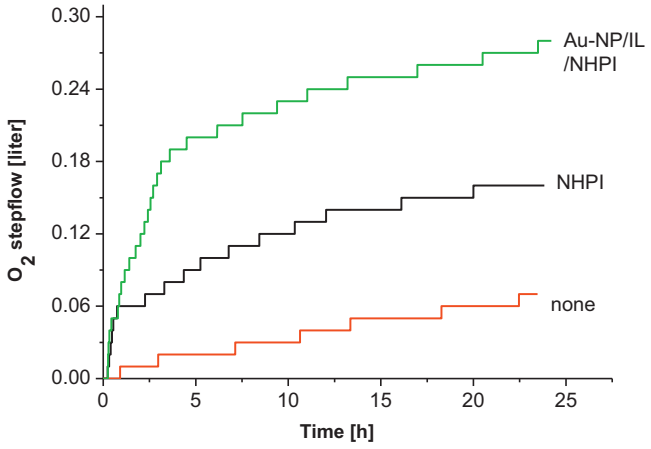

Fig. 3. Example curves (corresponding to Table 1, no. 7 (red), 8 (black) and 11 (green)) for the dioxygen gas uptake (volume at 4 bar pressure and 293 K ambient temperature) over time as a direct measure of the time–activity profile. (For interpretation of the references to color in this figure legend, the reader is referred to the web version of the article.)

selectivity (Table 1, nos. 5 and 6). Besides acetophenone also di(1-phenylethyl)ether and di(1-phenylethyl)peroxide were formed (Eq. (1)). Aliphatic and aromatic peroxides are used as curing agent for siloxane polymers [41]. A lower molar ratio of 1-phenylethanol to gold understandably increased the conversion (no. 6 versus no. 5).

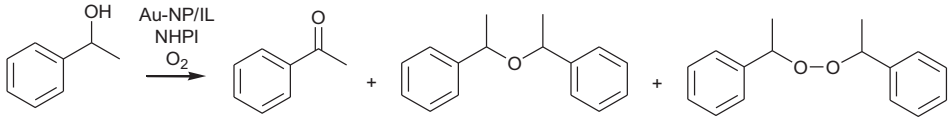

(1)

Oxidation of 1-phenylethanol with O_2/Au-NP was very sensitive to temperature. In the absence of the Au-NP catalyst oxidation proceeded up to 31% conversion with O_2 (Table 1, no. 7) or to 44% with O_2/NHPI only (no. 8) at 160 °C. The presence of Au-NP/IL (without NHPI) yielded a conversion of 50% at 160 °C (Table 1, no. 9) with about 70% selectivity for acetophenone. Increasing the amount of Au-NP/IL unexpectedly lowered the conversion (no. 10 versus no. 9) and also the selectivity. The highest conversion with TON of 5220 was achieved by Au-NP/IL/NHPI system (Table 1, no. 11). Using a higher amount of Au-NP in the Au-NP/IL/NHPI system again resulted in a lower conversion and selectivity (Table 1, no. 12). As part of our study we used various amounts of Au-NP/IL while keeping the NHPI amount (1 mmol) constant. With Au-NP/IL in any proportion relative to NHPI, the acetophenone selectivity always was lower than 100%. A near optimal condition in terms of acetophenone selectivity for the Au-NP/IL/NHPI system was obtained when 0.10 mL Au-NP/IL dispersion (with 6.1 μmol Au) was used with 1 mmol NHPI for 5.0 mL (41.35 mmol) 1-phenylethanol (entries nos. 5 and 11). Turnover numbers in oxidation reactions often start from less than 100 [42].

Except for the last two entries nos. 11 and 12 with the Au-NP/IL/NHPI system at 160 °C one can note an equimolar formation of di(1-phenylethyl)ether and di(1-phenylethyl)peroxide (Table 1) (see below for a suggested explanation).

The turnover number (TON) for metal nanoparticle catalyst is usually based on the number of moles of the metal used. Typically, only the surface atoms or even a fraction of it are catalytically active in a dispersed (heterogeneous) nanoparticle. Thus, the TON calculated from only the surface atoms can be one order of magnitude larger than the TON based on the total amount of metal for nanoparticles having more than 15 shells. Most likely, only a fraction of the surface atoms will be catalytically active, such as corners, edges or defect sites. Therefore, the TON based on surface atoms will still be an underestimate of the true, unknown TON [42].

From TEM and DLS we obtained an average Au-NP diameter of 8 nm. From this average nanoparticle diameter D the total number of metal atoms (N_T) in the nanocrystal can be calculated according to Eq. (2), (3) or (4):

$$N_T = \frac{N_A \rho V}{A_r} \quad \text{and} \quad V = \frac{4}{3}\pi\left(\frac{D}{2}\right)^3 \tag{2}$$

with N_A = Avogadro's number (6.022×10^{23} mol^{-1}), ρ = metal density, and A_r = relative atom mass (in g/mol) [42].

$$N_T = \frac{4\pi(D/2b)^3}{3V_g} \tag{3}$$

with b = 1.105 for closed packed (cp), face-centered cubic or hexagonal-cp (fcc or hcp) crystallographic structures and 1.137 for body-centered cubic (bcc) structures, V_g = volume of a single metal atom according to $V_g = (4/3)\pi r^3$, r = atomic (metal) radius. The formulae given in Ref. [42] and the supporting information of Ref. [43] (π missing there) are not denoted with b in the denominator. However, this constant b must be added there to account for the free space between the atom spheres in the metal packing.

$$N_T = \left(\frac{D}{2rb}\right)^3 \tag{4}$$

Eq. (4) is from Ref. [44] (given there as $d/d_{atom} = b(N_T)^{1/3}$).

With the values for gold (ρ = 19.32 g/cm^3, A_r = 196.966 g/mol, b = 1.105 for Au with fcc packing, V_g = 0.01256 nm^3, r = 0.1442 nm) Eq. (2), (3) or (4) give N_T = 15 820 atoms for Au-NP of 8 nm mean diameter.

The total average atom number N_T of 15 820 is close to the magic atom number of N_m = 14 993 for an icosahedron or cuboctahedron with m = 17 shells ($N_m = (1/3)(2m-1)(5m^2-5m+3)$) [45]. The number of surface atoms for a 17-shell icosahedron or cuboctahedron is N_S = 2562 ($N_S = 10m^2 - 20m + 12$) [45]. The fraction of exposed or surface atoms $N_S/N_T \approx 2560/15\,800$ is 0.16 or 16% on average. Thus, here the TON based on surface atoms will be a factor of about six larger than the TON based on the total number of moles of gold. In view of the Au-NP size dispersion the number of surface atoms, that is, their fraction can, however, only be an estimate.

For each reaction the dioxygen gas uptake was followed over time (Fig. 3). The gas uptake behavior with NHPI and Au-NP/IL/NHPI shows a high reactivity during the first 1 or 3 h, respectively. After this period, the curves level off. Yet, even after 24 h the reaction slowly continues. A comparison of the curve profiles and slow oxygen uptake in Fig. 3 after about 4–5 h is suggestive that after this time the catalyst activity of NHPI and Au-NP/IL/NHPI has mostly ceased and that the ongoing oxidation could be due to dioxygen alone. A gold catalyst poisoning might be responsible for the Au-NP/IL/NHPI plot leveling off. Such a poisoning could occur through coordination of oxygen or product species to the active gold sites (cf. Schemes 3 and 4).

For the Au-NP/IL catalytic systeme (without NHPI) work-up of the reaction mixture was carried out by vacuum distillation

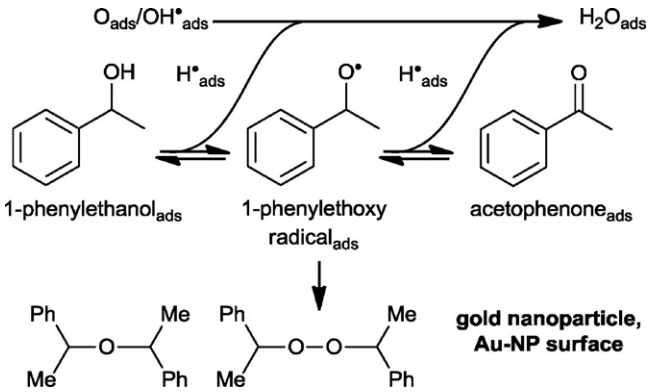

Scheme 3. Possible dehydrogenation mechanism [cf. 50,51] of 1-phenylethanol catalyzed on the metal surface by Au-NP/IL to form acetophenone as major product and the side products di(1-phenylethyl)ether and di(1-phenylethyl)peroxide (ads = adsorbed).

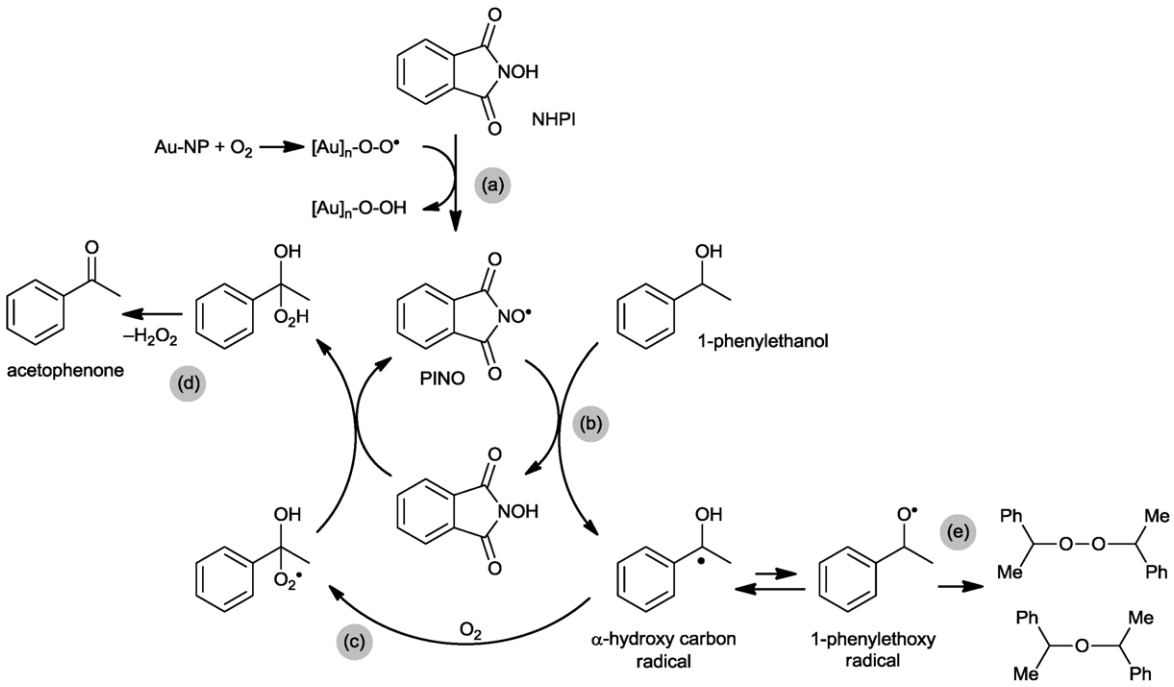

Scheme 4. Possible reaction pathways (adapted from Ref. [58]) for the aerobic oxidation of 1-phenylethanol catalyzed by Au-NP/IL/NHPI to form acetophenone as major product and the side products di(1-phenylethyl)ether and di(1-phenylethyl)peroxide. Steps (a)–(e) are described in the text.

(0.003 mbar, 200 °C) or by extraction with diethyl ether (3× 1 mL) in order to leave only the 0.1 mL Au-NP/IL dispersion in the reaction vessel and to test for recyclability. Fresh 1-phenylethanol substrate was then added but the conversion in the second run consistently reached at most only about 50% (160 °C, 4 bar) or about 25% (160 °C, 1 bar) of the conversion in the first run.

The consumed O_2 volumes in Fig. 3 agree with the observed conversions (Table 1) for the suggested mechanism (cf. Scheme 3) assuming ideal gas behavior for the calculation. The uptake of 0.07(1) L after 24 h for O_2 alone (without NHPI and Au-NP, red curve in Fig. 3) translates into 11.5(1.6) mmol O_2 which is to be compared with 31% conversion of 41.35 mmol alcohol into 12.8 mmol of products and H_2O_2. The O_2 uptake of 0.16(1) L after 24 h with NHPI (black curve in Fig. 3) corresponds to 26(2) mmol O_2 which is significantly higher than the 18.2 mmol products upon 44% conversion. This reflects additional O_2 needed for the NHPI-to-PINO (re)generation. The O_2 consumption of 0.28(1) L after 24 h with Au-NP/IL/NHPI (green curve in Fig. 3) equals 46(2) mmol, again more than 31.8 mmol products at 77% conversion due to additional O_2 for the PINO (re)generation.

The autoxidation of primary and secondary alcohol with dioxygen produces carbonyl compounds and hydrogen peroxide as the primary products (Scheme S1 in supporting information) [46]. Alcohols are generally not autoxidized as readily as olefins or aldehydes, mainly owing to the high rate of termination of α-hydroxy peroxy radicals.

Gold nanoparticles on solid supports are well known in alcohol oxidations, often under alkaline conditions, yet a mechanism is often not discussed and considered elusive [32,47]. A metal-assisted hydrogen abstraction from the hydroxyl group, which is favored under basic conditions, is seen as the initial step [48]. For example, it is generally accepted that benzaldehyde is formed from benzyl alcohol by dehydrogenation on the gold surface [49,50]. In the classical dehydrogenation mechanism on metal surfaces, the alcohol dehydrogenates in two steps. The adsorbed oxygen (O) or OH species react with the adsorbed H atoms (Scheme 3) [50,51]. The intermediate 1-phenylethoxy radical explains formation of the minor ether and peroxide products. Thermal desorption analysis on nanoporous gold confirmed the possible adsorptions of O_2 and 1-phenylethanol [28].

The efficient aerobic oxidation of various types of organic compounds has been carried out using *N*-hydroxyphthalimide (NHPI) as a key radical generator in recent years [52,53]. It is believed that the phthalimide *N*-oxyl (PINO) radical is generated in situ from the reaction of O_2 and NHPI [54]. In the presence of Au-NP the role of Au-NP probably lies in the activation of O_2 through chemisorption for the reaction with NHPI. The superoxo- or peroxo species, $[Au]_n$—O—O, facilitates the production of PINO similar to reported NHPI/Co(II) systems [55–57] (Scheme 4(a)).

Further, the PINO radical abstracts the hydrogen atom from 1-phenylethanol to produce the α-hydroxy carbon radical and regenerate NHPI (Scheme 4(b)). The resulting α-hydroxy carbon radical reacts with O_2 to form a peroxy radical (Scheme 4(c)), which is further converted to acetophenone, thereby regenerating the PINO radical from NHPI (Scheme 4(d)). A similar mechanism has been reported for the oxidation of alcohols to ketone or acid with O_2/NHPI/CuBr [58]. The PINO radical can, of course, also be regenerated through the reaction with Au-NP/O_2 (cf. Scheme 4(a)) or with O_2 alone in the absence of Au-NP which explains the higher O_2 consumption than is needed for the alcohol to ketone conversion alone (see above).

The α-hydroxy carbon radical in equilibrium with the 1-phenylethoxy radical can also react to the minor ether and peroxide products as sketched in Scheme 4(e). The largely equimolar formation of di(1-phenylethyl)ether and di(1-phenylethyl)peroxide suggests that they are coming from the same species. Since both the peroxide and ether are also produced in the absence of NHPI and Au-NP/IL at 160 °C (Table 1) and since there is no report on the formation of these products by the other metal-catalyzed oxidation of alcohols with NHPI/O_2 [52], we conclude that these compounds are produced because of partial stabilization of the 1-phenylethoxy radical in equilibrium with α-hydroxy carbon radical by the ionic liquid.

4. Conclusions

Gold nanoparticles in the ionic liquid 1-butyl-3-methylimidazolium tetrafluoroborate are active in the oxidation of phenylethanol to acetophenone with di(1-phenylethyl)ether $Ph(CH_3)CH{-}O{-}CH(CH_3)Ph$ and di(1-phenylethyl)peroxide $Ph(CH_3)CH{-}O{-}O{-}CH(CH_3)Ph$ as minor products. Good catalytic activities could, however, only be reached in the presence of the radical initiator *N*-hydroxyphthalimide (NHPI). While the IL stabilizes the Au-NP without the need for any additional capping ligands, it does so only in the absence of air. With O_2 the Au-NP continue to aggregate which will lead to deactivation, as does oxidation product coordination to active sites on the unprotected Au-NP surface. Furthermore, the IL can slow down a catalytic reaction due to mass transfer limitations [16] when compared to a solvent-free reaction or in organic solvents. Such a lower activity in IL than in no or in dichloroethane solvent has been reported for the epoxidation of cis-cyclooctene using dioxomolybdenum(VI) complexes and *tert*-butyl hydroperoxide [59]. Thus, we will now look into the use of supported, better recyclable and IL-free Au-NP@surface for oxidation catalysis following our work on highly active Ru-NP@graphene [5] and Rh-NP@Teflon [60] for hydrogenation catalysis.

Acknowledgment

This work was supported by DFG grant Ja466/23-1 (initiation of bilateral cooperation HHM-CJ).

Appendix A. Supplementary data

Supplementary data associated with this article can be found, in the online version, at http://dx.doi.org/10.1016/j.molcata.2013.02.007.

References

[1] G. Tojo, M. Fernandez, Oxidation of Alcohols to Aldehydes and Ketones, Springer, Berlin, 2006.
[2] J.E. Bäckvall (Ed.), Modern Oxidation Methods, Wiley-VCH, Weinheim, 2010.
[3] R.A. Sheldon, J.K. Kochi, Metal-Catalyzed Oxidation of Organic Compounds, Academic Press, New York, 1981.
[4] J. Dupont, J.D. Scholten, Chem. Soc. Rev. 39 (2010) 1780–1804.
[5] D. Marquardt, C. Vollmer, R. Thomann, P. Steurer, R. Mülhaupt, E. Redel, C. Janiak, Carbon 49 (2011) 1326–1332.
[6] D. Marquardt, Z. Xie, A. Taubert, R. Thomann, C. Janiak, Dalton Trans. 40 (2011) 8290–8293.
[7] S. Shylesh, V. Schünemann, W. Thiel, Angew. Chem. Int. Ed. 49 (2010) 3428–3459.
[8] O.T. Mefford, M.L. Vadala, J.D. Goff, M.R.J. Caroll, R. Mejia-Ariza, B.L.T.G. Caba, St. Pierre, R.C. Woodward, R.M. Davis, J.S. Riffle, Langmuir 24 (2008) 5060–5069.
[9] (a) D. Astruc, F. Lu, J.R. Aranzaes, Angew. Chem. Int. Ed. 44 (2005) 7852–7872; (b) C. Pan, K. Pelzer, K. Philippot, B. Chaudret, F. Dassenoy, P. Lecante, M.-J. Casanove, J. Am. Chem. Soc. 123 (2001) 7584–7593; (c) J.D. Aiken III, R.G. Finke, J. Am. Chem. Soc. 121 (1999) 8803–8810.
[10] K. Ueno, H. Tokuda, M. Watanabe, Phys. Chem. Chem. Phys. 12 (2010) 1649–1658.
[11] (a) J. Dupont, J. Brazil. Chem. Soc. 15 (2004) 341–350; (b) M.-A. Neouze, J. Mater. Chem. 20 (2010) 9593–9607; (c) C.S. Consorti, P.A.Z. Suarez, R.F. de Souza, R.A. Burrow, D.H. Farrar, A.J. Lough, W. Loh, L.H.M. da Silva, J. Dupont, J. Phys. Chem. B 109 (2005) 4341–4349; (d) J. Dupont, P.A.Z. Suarez, R.F. de Souza, R.A. Burrow, J.-P. Kintzinger, Chem. Eur. J. 6 (2000) 2377–2381.
[12] (a) E. Redel, M. Walter, R. Thomann, C. Vollmer, L. Hussein, H. Scherer, M. Krüger, C. Janiak, Chem. Eur. J. 15 (2009) 10047–10059; (b) E. Redel, M. Walter, R. Thomann, L. Hussein, M. Krüger, C. Janiak, Chem. Commun. 46 (2010) 1159–1161.
[13] (a) L. Durán Pachón, G. Rothenberg, Appl. Organomet. Chem. 22 (2008) 288–299; (b) A. Gual, C. Godard, S. Castilló, C. Claver, Dalton Trans. 39 (2010) 11499–11512.
[14] V.I. Pârvulescu, C. Hardacre, Chem. Rev. 107 (2007) 2615–2665.
[15] D. Betz, P. Altmann, M. Cokoja, W.A. Herrmann, F.E. Kühn, Coord. Chem. Rev. 255 (2011) 1518–1540.
[16] J.D. Scholten, B.C. Leal, J. Dupont, ACS Catal. 2 (2012) 184–200.
[17] R.A. Sheldon, Chem. Commun. (2008) 3352.
[18] (a) P. Wasserscheid, T. Welton, Ionic Liquid in Synthesis, vol. 1, Wiley-VCH, Weinheim, 2007, pp. 32–61, 325; (b) C. van Doorslaer, Y. Schellekens, P. Mertens, K. Binnemanns, D. De Vos, Phys. Chem. Chem. Phys. 12 (2010) 1741.
[19] K.R. Seddon, A. Stark, Green Chem. 4 (2002) 119–123.
[20] (a) A.S.K. Hashmi, Top. Organomet. Chem. 44 (2013) 143–164; (b) A.S.K. Hashmi, T. Wang, S. Shi, M. Rudoph, J. Org. Chem. 77 (2012) 7761–7767; (c) A.S.K. Hashmi, M.C. Blanco Jaimes, A.M. Schuster, F. Rominger, J. Org. Chem. 77 (2012) 6394–6408; (d) A.S.K. Hashmi, Chem. Rev. 107 (2007) 3180–3211.
[21] C. Della Pina, E. Falletta, M. Rossi, Chem. Soc. Rev. 41 (2012) 350–369.
[22] J.L. Gong, C.B. Mullins, Acc. Chem. Res. 42 (2009) 1063–1073.
[23] G.C. Bond, D.T. Thompson, Catal. Rev. Sci. Eng. 41 (1999) 319–388.
[24] L. Prati, M. Rossi, J. Catal. 176 (1998) 552–560.
[25] S. Biella, M. Rossi, Chem. Commun. (2003) 378–379.
[26] C. Della Pina, E. Falletta, L. Prati, M. Rossi, Chem. Soc. Rev. 37 (2008) 2077–2095.
[27] M. Boualleg, K. Guillois, B. Istria, L. Burel, L. Veyre, J.-M. Basset, C. Thieuleux, V. Caps, Chem. Commun. 46 (2010) 5361–5363.
[28] N. Asao, N. Hatakeyama, Menggenbateer, T. Minato, E. Ito, M. Hara, Y. Kim, Y. Yamamoto, M. Chen, W. Zhang, A. Inoue, Chem. Commun. 48 (2012) 4540–4542.
[29] C.-H. Liu, Y. Guan, E.J.M. Hensen, J.-F. Lee, C.-M. Yang, J. Catal. 282 (2011) 94–102.
[30] T. Punniyamurthy, S. Velusamy, J. Iqbal, Chem. Rev. 105 (2005) 2329–2363.
[31] M. Chen, Y. Cai, Z. Yan, D.W. Goodman, J. Am. Chem. Soc. 128 (2006) 6341–6346.
[32] (a) V.R. Choudhary, A. Dhar, P. Jana, R. Jha, B.S. Uphade, Green Chem. 7 (2005) 768–770; (b) V.R. Choudhary, R. Jha, P. Jana, Green Chem. 9 (2007) 267–272.
[33] R.A. Sheldon, I.W.C.E. Arends, G.-J. Brink, A. Dijksman, Acc. Chem. Res. 35 (2002) 774–781.
[34] Z. Shi, C. Zhang, C. Tang, N. Jiao, Chem. Soc. Rev. 41 (2012) 3381–3430.
[35] F. Endres, S.Z. El Abedin, Phys. Chem. Chem. Phys. 8 (2006) 2101–2116.
[36] R.P. Swatloski, J.D. Holbrey, R.D. Rogers, Green Chem. 5 (2003) 361–363.
[37] G.A. Baker, S.N. Baker, Aust. J. Chem. 58 (2005) 174–177.
[38] H. Hachenberg, K. Beringer, Die Headspace-Gaschromatographie als Analysen- und Meßmethode, Vieweg, Braunschweig/Wiesbaden, Germany, 1996, pp. 32–35.
[39] J.D. Scholten, G. Ebeling, J. Dupont, Dalton Trans. (2007) 5554–5560.
[40] P.J. Barnard, M.V. Baker, S.J. Berners-Price, B.W. Skelton, A.H. White, Dalton Trans. (2004) 1038–1047.
[41] D.R. Thomas, Siloxane Polymers, Prentice Hall, Englewood Cliffs, NJ, 1993, pp. 567–615.
[42] A.P. Umpierre, E. de Jesús, J. Dupont, ChemCatChem 3 (2011) 1413–1418.
[43] O.M. Wilson, M.R. Knecht, J.C. Garcia-Martinez, R.M. Crooks, J. Am. Chem. Soc. 128 (2006) 4510–4511.
[44] A. Borodzinski, M. Bonarowska, Langmuir 13 (1997) 5613–5620.
[45] R.E. Benfield, J. Chem. Soc. Faraday Trans. 88 (1992) 1107–1110.
[46] E.T. Denisov, N.I. Mitskevich, V.E. Agabekov, Liquid Phase Oxidation of Oxygen-Containing Compounds (D.A. Paterson, Engl. Transl.), Consultants Bureau, New York, 1977, p. 23.
[47] H. Li, B. Guan, W. Wang, D. Xing, Z. Fang, X. Wan, L. Yang, Z. Shi, Tetrahedron 63 (2007) 8430–8434.
[48] S. Biella, G.L. Castiglioni, C. Fumagalli, L. Prati, M. Rossi, Catal. Today 72 (2002) 43–49.
[49] K. Chen, H. Wu, Q. Hua, S. Chang, W. Huang, Phys. Chem. Chem. Phys. 15 (2013) 2273–2277.
[50] M. Besson, P. Gallezot, Catal. Today 57 (2000) 127–141.
[51] T. Mallat, A. Baiker, Chem. Rev. 104 (2004) 3037–3058.
[52] Y. Ishii, S. Sakaguchi, T. Iwahama, Adv. Synth. Catal. 343 (2001) 393–427.
[53] A. Dhakshinamoorthy, M. Alvaro, H. Garcia, Catalysis 1 (2011) 836–840.
[54] T. Iwahama, Y. Yoshino, T. Keitoku, S. Sakaguchi, Y. Ishii, J. Org. Chem. 65 (2000) 6502–6507.
[55] C.L. Wong, J.A. Switer, K.P. Balakrishnan, J.F. Endicott, J. Am. Chem. Soc. 102 (1980) 5511–5518.
[56] R.S. Drago, J.P. Cannady, K.A. Leslie, J. Am. Chem. Soc. 102 (1980) 6014–6019.
[57] L.I. Simándi, Catalytic Activation of Dioxygen by Metal Complexes, Kluwer Academic, Dordrecht, 1992, pp. 1–73, and references cited therein.
[58] G. Yang, L. Wang, J. Li, Y. Zhang, X. Dong, Y. Lv, S. Gao, Res. Chem. Intermed. 38 (2012) 775–783.
[59] A.A. Valente, Ž. Petrovski, L.C. Branco, C.A.M. Afonso, M. Pillinger, A.D. Lopes, C.C. Romão, C.D. Nunes, I.S. Gonçalves, J. Mol. Catal. A: Chem. 218 (2004) 5–11.
[60] C. Vollmer, M. Schröder, Y. Thomann, R. Thomann, C. Janiak, Appl. Catal. A 425–426 (2012) 178–183.